

# Single cell recordings with pairs of complementary transistors

Sven Meyburg, Günter Wrobel, Regina Stockmann, Jürgen Moers,  
Sven Ingebrandt, and Andreas Offenhäuser<sup>a)</sup>

*Institute of Bio- and Nanosystems and Center of Nanoelectronic Systems for Information Technology (CNI),  
Research Center Jülich, D-52425 Jülich, Germany*

(Received 7 April 2006; accepted 19 May 2006; published online 6 July 2006)

Floating gate field-effect transistors (FETs) for the detection of extracellular signals from electrogenic cells were fabricated in a complementary metal oxide semiconductor process. Additional passivation layers protected the transistor gates from the electrolyte solution. To compare the signals from *n*- and *p*-FETs, two electronically separated, but locally adjacent transistors were combined to one measuring unit. The paired sensing area of this unit had the dimension of a single cell. Simultaneous recordings with *n*- and *p*-channel floating gate FETs from a single cell exhibited comparable amplitudes and identical time courses. The experiments indicate that both types of FETs express similar sensitivities. © 2006 American Institute of Physics. [DOI: [10.1063/1.2219339](https://doi.org/10.1063/1.2219339)]

Recording extracellular electrical activity from living cells with semiconductor devices is a powerful tool that holds great promise for biomedical and neuroelectronic applications as well as for the development of whole-cell biosensors. In contrast to classical electrophysiological methods, these devices allow stable long-term, noninvasive recordings of electrical activity from single cells or networks of cells with multiple recording sites. For extracellular recordings, two main concepts were developed in the past: multielectrode arrays<sup>1,2</sup> (MEAs) with metallized contacts and field-effect transistor<sup>3,4</sup> (FETs) arrays. When using FETs, the gate oxide provides a high impedance input. The presented FET designs had either nonmetallized, oxidic gates (also called open gates)<sup>4,5</sup> or metallized gates. The latter were either in direct contact to the electrolyte solution<sup>6,7</sup> or had electrically insulated, so-called floating gates.<sup>8–10</sup>

In recent works, we examined the extracellular recordings of a human embryonic kidney cell line (HEK293) expressing a voltage-gated  $K^+$  channel using either nonmetallized, open-gate *n*- or *p*-channel FETs.<sup>11</sup> In general, these extracellular signals showed distinct differences. The *n*-FET signals were significantly larger in amplitude and we observed a slower time course compared to the *p*-FET signals. In order to investigate these discrepancies, we developed a pair of electronically separated, but locally adjacent floating gate *n*- and *p*-FETs for the recording of extracellular signals in this work. Each of these sensing units exposed a paired sensing area with the dimension of a single cell. This sensing area was isolated from the electrolyte solution by a thin, thermally grown oxide.

The fabrication process of our floating gate field-effect transistors (FGFETs) was partially adopted from a twin-well, 1.3  $\mu\text{m}$ , double polycrystalline silicon, double metal complementary metal oxide semiconductor (CMOS) process of the Microfabrication Laboratory, University of California at Berkeley.<sup>12</sup> After the self-aligned drain-source implantations the wafers were covered with 550 nm silicon dioxide, deposited by standard low-pressure chemical vapor deposition (LPCVD). Drain and source contacts as well as contacts to the lower gate layer—outside the active area of the

transistor—were opened by reactive ion etching (RIE). A layer of 150 nm *n*-doped polycrystalline silicon was deposited (LPCVD) to form the interconnects and the upper part of the paired floating gate, the sensing area. The layer was structured by RIE and the interconnects were silicided with titanium to decrease the access resistance. The wafers were passivated with 100 nm silicon dioxide by plasma enhanced chemical vapor deposition (PECVD), 150 nm silicon nitride (LPCVD), and 100 nm silicon dioxide (LPCVD). The sensing area was opened by RIE and thermally oxidized by rapid thermal processing for 10 min at 800 °C. Finally, Ti/Au bond pads were defined by a lift-off process. Our FGFET design combined a CMOS-type transistor optimized for high transconductance and low noise with an independent sensing area that was adapted to the size of an adhering cell.<sup>10</sup> Ions like sodium or potassium penetrating into the gate oxide are known to deteriorate the properties of open-gate FETs. The design of the floating gate transistor protects the gate oxide from the electrolyte solution and enables multiple reuse of the devices. Each chip contained an array of eight of *n*- and *p*-channel FET units. They were mounted on standard 40 pin dual-inline ceramic chip carriers, wire bonded, and partially encapsulated to form a culture dish on the device.<sup>5,10</sup> Details of the amplifier system for the FETs have been described elsewhere.<sup>13</sup> Figure 1(a) shows a cross section and Fig. 1(b) a top view of a measuring unit and the paired sensing area.

We cultured HEK293 cells expressing a voltage-gated ether-à-gogo (EAG) potassium channel<sup>11</sup> on the FET chips. The activation kinetics of this ion channel is well known and depends on the stimulation pulse and the concentrations of divalent cations.<sup>14–16</sup> The FET chips were cleaned<sup>5,11</sup> and coated with poly(L)lysine (Sigma). The cell culture was adapted from previously published protocols.<sup>11</sup> After cell plating, the chips were incubated at 37 °C and 5% CO<sub>2</sub> for three to five days.

Cells that covered the sensing unit [Fig. 1(c)] were attached by a patch pipette in the whole-cell configuration, and rectangular voltage pulses were applied. The membrane current  $I_M$  and the corresponding *n*- and *p*-channel FET signals were recorded simultaneously. The changes in the drain-source current  $I_{DS}$  are correlated with changes in the gate voltage of the FET ( $V_{FET}$ ), as given by  $\Delta V_{FET} = \Delta I_{DS} / g_m$ .<sup>17,18</sup>  $V_{FET}$  of both transistors was ampli-

<sup>a)</sup> Author to whom correspondence should be addressed; FAX: +49 2461 61-8733; electronic mail: [a.offenhaeuser@fz-juelich.de](mailto:a.offenhaeuser@fz-juelich.de)

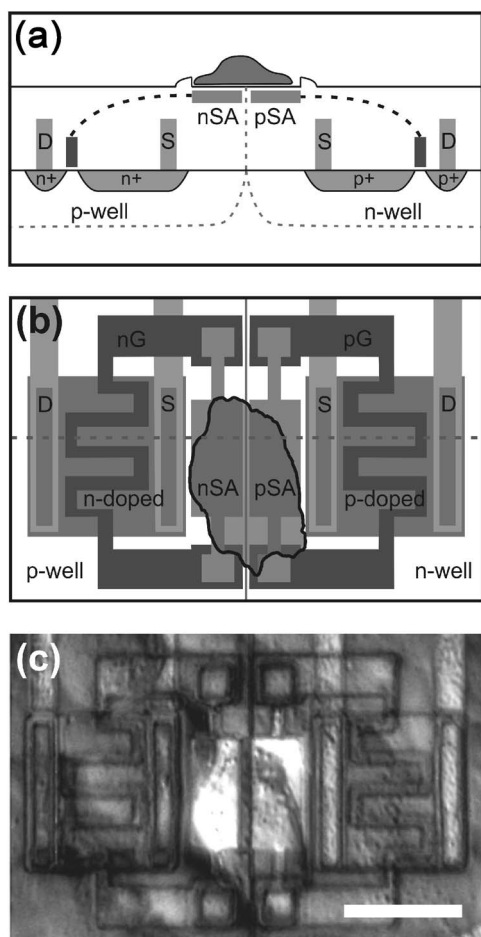


FIG. 1. Schematic cross section (a) and top view (b) of a measuring unit consisting of two electronically separated, but locally adjacent *n*- and *p*-FGFETs and the corresponding paired sensing area. The position of the cross section is indicated in (b) by a dotted line. Source and drain are labeled S and D; gates are labeled nG for the *n*-FGFET and pG for the *p*-FGFET. The sensing areas are labeled nSA and pSA, respectively. The black dotted line in (a) indicates the connection between the sensing area and the respective gate. (c) Microscopic image of HEK293 cells on a poly(L)lysine coated chip surface after four days in culture. The position of the particular cell on the paired sensing area is schematically shown in (b). Scale bar=20 μm.

fied and fed into an EPC-10 patch-clamp amplifier (HEKA Elektronik). The patch pipettes were filled with an intracellular solution (in millimolar: 125 KCl, 2 MgCl<sub>2</sub>, 10 EGTA, 10 HEPES, 5 Na-ATP, adjusted to pH of 7.4 with KOH). The extracellular solutions were (in millimolar) 5 KCl, 140 NaCl, 1 CaCl<sub>2</sub>, 5 MgCl<sub>2</sub>, 10 HEPES, 5 glucose, adjusted to pH of 7.4 with NaOH. A Ag/AgCl electrode, which was set to ground potential, served as reference electrode for both FETs and the patch-clamp amplifier.

Figure 2(a) shows a typical recording of the transmembrane whole-cell potassium current  $I_M$  from a HEK293 cell. The time course of  $I_M$  displayed the same characteristics as previously described for EAG currents.<sup>11,14–16</sup> Figure 2(b) shows the corresponding *n*- and *p*-channel FET recordings. A quasilinear drift of the FET signals during the recording was subtracted. The root-mean-square noise was 52 μV for the *n*-channel and 67 μV for the *p*-channel FET in this particular recording. In order to enhance the signal-to-noise ratio, the recordings were averaged ( $n=50$  traces). The time courses of all FET signals were the same for both types of FET ( $n=14$  cells). They resemble a combination of different signal components, which were already previously

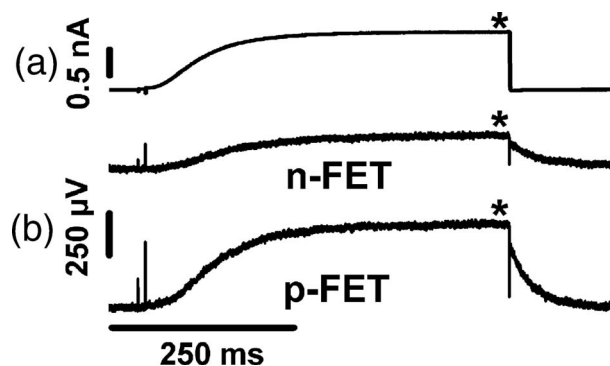


FIG. 2. Typical whole-cell membrane current  $I_M$  (a) and the corresponding averaged *n*- and *p*-channel FGFET recordings  $V_{FET}$  (b) for a membrane depolarization from −70 to +50 mV. The stars indicate the steady-state  $I_M$  and  $V_{FET}$  amplitudes.

described:<sup>11</sup> (i) capacitive transients at the onset and offset of the voltage stimulus, caused by capacitive coupling of the stimulus through the attached membrane,<sup>17–19</sup> (ii) an increase of  $V_{FET}$  to a steady-state amplitude, (iii) a partially instantaneous decline of  $V_{FET}$  at the end of the stimulus (Ohmic coupling), and (iv) a slower relaxation of  $V_{FET}$ , that is not observed for  $I_M$  (electrochemical coupling). In all recorded signals, the amplitude for *n*- and *p*-FETs differed from each other, whereas the time course was always the same for both transistor signals. Figure 3 shows a comparison of the steady-state amplitudes of our extracellular recordings using the pairs of *n*- and *p*-FETs. For  $n=14$  cells we recorded amplitudes of  $92 \pm 63$  μV for the *n*-FETs and higher values of  $140 \pm 121$  μV for the *p*-FETs. A t-test on all steady-state FET recordings [see “\*” in Fig. 2(b)] resulted in a *p*-value of  $p=0.20$ . In conclusion, the *n*- and *p*-FET signal amplitudes do not differ significantly. The large standard deviations of the amplitudes in Fig. 3 can be explained by unequal coverage of the respective sensing areas by the cells.

In a previous study with open-gate FETs, we found that the amplitudes of *n*-FET signals were significantly larger than those for *p*-FETs. Moreover, the signal relaxation was slower for the *n*-FETs. These differences were discussed as an effect of slightly different ion sensitivities of both chip types.<sup>11</sup> It was already discussed that the selective ion binding to the silicon oxide could also influence the recorded signal shapes.<sup>20</sup> In the present study, the transistors used for the individual measurements were situated on the same chip, and therefore differences in the respective surface properties of the paired gate can be excluded. In order to compare the time course of the FET signals, we normalized the traces with respect to their steady-state amplitude. Figure 4 shows a comparison of normalized *n*- (black traces) and *p*-FET recordings (gray traces) with different contributions of the

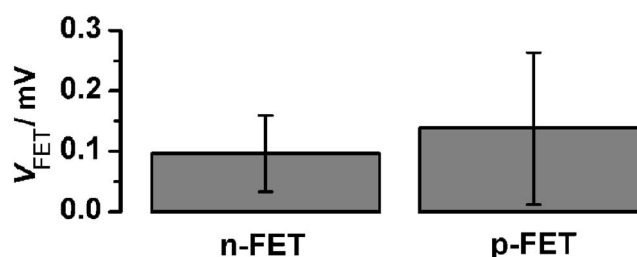


FIG. 3. Average of the steady-state signal amplitudes of the *n*- and *p*-channel FGFET recordings ( $n=14$  cells).

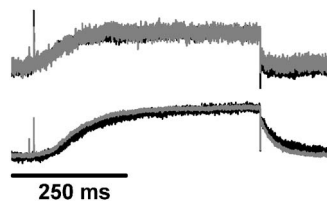


FIG. 4. Two typical time courses of FET signals recorded with pairs of  $n$ - (black traces) and  $p$ -FGFETs (gray traces). The signals were normalized with respect to their steady-state amplitude.

slow relaxation component. Although the signal shapes recorded by pairs of FETs differed from experiment to experiment, all simultaneously recorded signals with adjacent  $n$ - and  $p$ -channel FETs had identical time courses. These results support the assumption that formerly recorded differences in the FET signals might be related to differences in the surface properties of  $n$ - and  $p$ -FETs, respectively.<sup>11</sup>

In conclusion, we built pairs of  $n$ - and  $p$ -channel floating-gate FETs in a 1.3  $\mu\text{m}$  twin-well, two polycrystalline silicon layer CMOS process. Simultaneous recording of extracellular signals from single cells has been demonstrated. The  $n$ - and  $p$ -FET signals showed identical time courses in their respective signal components.

The authors thank R. Otto and N. Wolters (ISG-2) for the technical support with the FET amplifier system. They also thank H. Lüth (ISG-1) and A. Steffen (ISG-PT) for the support with the chip development and fabrication. The authors gratefully thank A. Baumann (IBI-1) for stably transforming the HEK293 cells with the *beag1* gene and providing them with this cell line. The HEK293 recordings were done in collaboration with the group of U. B. Kaupp (IBI-1, all For-

schungszentrum Jülich). This work was partially funded by the Volkswagen Stiftung.

<sup>1</sup>J. Pine, J. Neurosci. Methods **2**, 19 (1980).

<sup>2</sup>G. W. Gross, W. Y. Wen, and J. W. Lin, J. Neurosci. Methods **15**, 243 (1985).

<sup>3</sup>P. Bergveld, J. Wiersma, and H. Meertens, IEEE Trans. Biomed. Eng. **23**, 136 (1976).

<sup>4</sup>P. Fromherz, A. Offenhäusser, T. Vetter, and J. Weis, Science **252**, 1290 (1991).

<sup>5</sup>A. Offenhäusser, C. Sprössler, M. Matsuzawa, and W. Knoll, Biosens. Bioelectron. **12**, 819 (1997).

<sup>6</sup>D. T. Jobling, J. G. Smith, and H. V. Wheal, Med. Biol. Eng. Comput. **19**, 553 (1981).

<sup>7</sup>M. S. Brenner, Ph.D. thesis, Technische Universität München, 2001.

<sup>8</sup>A. Offenhäusser, J. Rühle, and W. Knoll, J. Vac. Sci. Technol. A **13**, 2606 (1995).

<sup>9</sup>A. Cohen, M. E. Spira, S. Yitshaik, G. Borghs, O. Shwartzglass, and J. Shappir, Biosens. Bioelectron. **19**, 1703 (2004).

<sup>10</sup>S. Meyburg, M. Goryll, J. Moers, S. Ingebrandt, S. Böcker-Meffert, H. Lüth, and A. Offenhäusser, Biosens. Bioelectron. **21**, 1037 (2006).

<sup>11</sup>G. Wrobel, R. Seifert, S. Ingebrandt, J. Enderlein, H. Ecken, A. Baumann, U. B. Kaupp, and A. Offenhäusser, Biophys. J. **89**, 3628 (2005).

<sup>12</sup>BASILINE CMOS PROCESS (4"), Version 5.0, 1997; <http://microlab.berkeley.edu>

<sup>13</sup>S. Meyburg, Ph.D. thesis, Rheinisch-Westfälische Technische Hochschule Aachen, 2005.

<sup>14</sup>H. Terlau, J. Ludwig, R. Steffan, O. Pongs, W. Stühmer, and S. H. Heinemann, Pfluegers Arch. **432**, 301 (1996).

<sup>15</sup>R. Schönherr, L. M. Mannuzzu, E. Y. Isacoff, and S. H. Heinemann, Neuron **35**, 935 (2002).

<sup>16</sup>S. Frings, N. Brüll, C. Dzeja, A. Angele, V. Hagen, U. B. Kaupp, and A. Baumann, J. Gen. Physiol. **111**, 583 (1998).

<sup>17</sup>R. Schätzthauer and P. Fromherz, Eur. J. Neurosci. **10**, 1956 (1998).

<sup>18</sup>C. Sprössler, M. Denyer, S. Britland, A. Curtis, W. Knoll, and A. Offenhäusser, Phys. Rev. E **60**, 2171 (1999).

<sup>19</sup>S. Ingebrandt, C. K. Yeung, M. Krause, and A. Offenhäusser, Eur. Biophys. J. **34**, 144 (2005).

<sup>20</sup>M. Brittinger and P. Fromherz, Appl. Phys. A: Mater. Sci. Process. **81**, 439 (2005).